UNIVERSITÀ DEGLI STUDI DI MILANO

FACOLTÀ DI SCIENZE E TECNOLOGIE

Bachelor's Degree in Physics

Next-to-Leading Order QCD Corrections to Scattering Processes Using θ-Parameters in the Nested Soft-Collinear Subtraction Scheme

Supervisor:
Prof. Raoul Horst Röntsch

Student:
Lucrezia Bioni
Matr.: 13655A

Academic Year 2024–2025

Abstract

Quantum Chromodynamics (QCD) corrections at next-to-leading order (NLO) are an essential component of high-precision theoretical predictions in high-energy particle physics. The nested soft-collinear subtraction (NSC) scheme provides an established framework for computing these corrections, offering an efficient method for handling infrared (IR) divergences through a nested factorization of soft and collinear singularities. This approach ensures proper cancellation of divergences. In this work, we focus on hadronic scattering processes and we extend the NSC framework by implementing θ-parameters, which systematically restrict the subtraction procedure to the singular, unresolved regions of phase space. This refinement is designed to further enhance the scheme's numerical stability and computational efficiency by optimizing the treatment of IR-sensitive contributions.

Contents

1 Introduction **1**
1.1 The Standard Model . . . 1
1.1.1 Collider physics . . . 1
1.2 QCD and hard scattering processes . . . 2
1.2.1 Hadronic cross-section and factorization theorem . . . 2
1.2.2 Partonic cross-section . . . 5
1.2.3 Infrared poles and their cancellation . . . 7
1.2.4 The origin of infrared divergences in real-emission contributions . . . 7

2 NLO QCD corrections in the NSC Subtraction Scheme **10**
2.1 Draft . . . 10

3 NLO QCD corrections with θ-parameters in the NSC Subtraction Scheme **11**
3.1 Draft . . . 11

Appendices **12**

A Draft appendix **14**
A.1 Draft . . . 14

Bibliography **15**

Chapter 1

Introduction

§1.1 The Standard Model

As Aristotle stated, women and men began to philosophize due to wonder. From antiquity, a profound sense of astonishment towards the natural world has driven humans to investigate phenomenological reality. This drive is so profound and innate in humanity that – starting with the first philosophers, called "Pre-Socratics" or "natural philosophers" – it led them to inquire into the nature of the "archè" (ἀρχή), the primordial principle and fundamental constituent underlying all of nature. This enduring pursuit of fundamental knowledge evolved through the centuries and, in the last one, culminated in the experimental discovery of a multitude of subatomic particles, now understood to be the elementary constituents of matter. Their proliferation was such that it prompted the noted physicist Enrico Fermi to remark: "If I could remember the names of all these particles, I'd be a botanist". This apparent complexity, however, has been successfully resolved through the development of a robust theoretical framework that classifies these particles and describes their interactions via gauge theories: the Standard Model (SM).
The SM is formulated within the mathematical framework of Quantum Field Theory (QFT), which unifies the principles of Quantum Mechanics and Special Relativity to describe phenomena at high energies and subatomic scales. Its predictions have been rigorously tested and confirmed by experiments, most notably with the discovery of the Higgs boson in 2012. Despite its success, there are significant efforts to discover Physics beyond the SM. This is driven not only by the natural attempt at falsification that should be applied to every scientific theory, but also by several phenomena that the model cannot explain. These include the existence of dark matter and dark energy, the observed matter-antimatter asymmetry, and the origin of neutrino masses [11].

§1.1.1 Collider physics

The principal method of research in high-energy physics is collider physics [5]. Using colliders, it is possible to artificially accelerate particles and reach the highest available center-of-mass energy. Operating at the energy frontier is crucial: higher-energy collisions enable events with greater momentum transfer and energy deposition. These events are essential because concentrating significant energy within a tiny volume allows us to excite new, heavy elementary particles from the vacuum, and study their properties. Experiments at the energy frontier are conducted at the Large Hadron Collider (LHC) at CERN: in a 27-kilometer ring, proton beams

collide at a center-of-mass energy of 13 TeV. Although these energy scales have allowed us to study the known fundamental interactions – with the exception of gravity – in great detail, they have not been sufficient for the discovery of new particles. Since increasing the energy of the colliding particles is not feasible with existing technology, the focus of collider experiments in the next decade will shift towards higher experimental precision. However, testing the Standard Model with experimental results necessitates reliable theoretical predictions for hadron collider processes.

§1.2 QCD and hard scattering processes

A theoretical description of hadron collisions is complicated primarily by our limited knowledge of the strong force, which binds the elementary constituents of hadrons. A way to overcome this obstacle becomes manifest when we consider how hadrons collide at high energies [13]. Typically, they undergo either elastic scattering or diffractive dissociation: in the first case, they collide but remain intact; in the second, they disintegrate into a small number of hadrons. However, on rare occasions, a more interesting phenomenon can occur: the elementary partons that compose the hadrons can interact and exchange a large amount of momentum. This is the case in so-called "hard scattering processes", and their importance is related to a significant feature of the strong force: asymptotic freedom. The essence of this property is the weakening of the colour force at short distances [5], which is precisely what allows for a perturbative description of the strong interaction and the use well-defined approximation methods. Therefore, in these cases, it is possible to organize the calculation into different orders:

- the Leading Order (LO), which describes the simplest, tree-level interaction;
- the Next-to-Leading Order (NLO), which adds important quantum corrections from virtual particle loops and the emission of an additional parton (real radiation);
- the Next-to-Next-to-Leading Order (NNLO), which includes two-loop, one-loop with real emission, and double real-emission diagrams; and so on.

§1.2.1 Hadronic cross-section and factorization theorem

Strong interactions are described by Quantum Chromodynamics (QCD), a non-abelian gauge theory based on the SU(3) symmetry group. Their strength is given by the coupling constant, which is on the order of $\alpha_S \sim 0.1$[1]: therefore, the strong force is about ten times stronger than the electromagnetic one (whose coupling constant is $\alpha \sim 1/137$). The QCD Lagrangian is not analytically solvable, making it extremely difficult to understand proton dynamics from first principles. Therefore, an approach that focuses on the elementary quark and gluon fields, which are the fundamental degrees of freedom in QCD, is highly valuable. However, due to quark confinement[2], this approach is only sensible at short distances. In this high-energy regime, the interacting partons can be approximated as being nearly free.

[1] This value is energy-dependent; $\alpha_S \sim 0.1$ is typical at energies around 100 GeV.

[2] Quark confinement is the phenomenon that prevents quarks and gluons from propagating as free particles over macroscopic distances.

A framework for describing these short-distance hard scattering processes is provided by the collinear factorization theorem [4]. Within this framework, colliding hadrons are treated as beams of partons, each carrying a certain fraction of the hadron's total momentum. The probability of finding a parton with a specific energy fraction is encoded in the Parton Distribution Functions (PDFs). These functions are universal, meaning they are independent of the specific scattering process being studied. Consequently, PDFs can be measured in one set of experiments and then used to make predictions for many others [12]. The short-distance interaction of partons produces final states composed of Standard Model particles, such as leptons, gauge bosons, and additional QCD partons. The final-state partons, which are the direct products of the perturbative calculation, cannot be observed directly due to confinement. Instead, they evolve into collimated sprays of hadrons [8]. We interpret these partons as the seeds of hadronic jets and define the resulting sprays as jets themselves. At high energies, the properties of these jets are largely determined by the perturbative dynamics of their initiating parton and are only mildly affected by non-perturbative QCD effects.
The production cross section for final states involving QCD jets and other Standard Model particles in hard hadronic collisions is thus given by

$$\mathrm{d}\sigma = \sum_{a,b} \int_0^1 \mathrm{d}x_1 \mathrm{d}x_2\, f_a(x_1, \mu_\mathrm{F})\, f_b(x_2, \mu_\mathrm{F})\, \mathrm{d}\hat{\sigma}_{a,b}(x_1, x_2, \mu_\mathrm{F}, \mu_\mathrm{R}; \mathcal{O}) \left(1 + \mathcal{O}\left(\frac{\Lambda_\mathrm{QCD}}{Q}\right)^n\right), \qquad n \geq 1 \tag{1.1}$$

where $f_{a,b}$ are the parton distribution functions mentioned above, and $\mathcal{O}$ is an infrared-finite observable.
The asymptotic freedom of QCD is what enables a perturbative description of the strong interaction. However, it is crucial to recognize that the precise mechanism allowing us to decouple the motion of partons from the proton's dynamics is the separation of energy scales involved. Interactions in the Standard Model typically probe energy scales on the order of $Q \sim 100\,\mathrm{GeV} - 1\,\mathrm{TeV}$, while the characteristic energy scale of hadronic structure and confinement is significantly lower, $\Lambda_\mathrm{QCD} \sim 100\,\mathrm{MeV}$. This results in a small ratio, $\Lambda_\mathrm{QCD}/Q \sim 10^{-2}$. The exact power n with which non-perturbative effects are suppressed is not always immediately evident. In many practical applications, the leading power is $n = 2$, implying that the theoretical error committed by factorizing the non-perturbative physics is of order $\mathcal{O}(\alpha_\mathrm{S}^4) \sim 10^{-3}$ for $\alpha_S \sim 0.1$.
This formalism establishes a clear distinction between the short-distance perturbative process and the long-distance non-perturbative physics. The boundary between these two regimes is defined by the factorization scale (μ_F). Processes with a momentum transfer $Q > \mu_\mathrm{F}$ are treated as the hard scatter of point-like partons, calculable within perturbation theory. Physics at scales $Q < \mu_\mathrm{F}$, which describes how the partons are bound within the proton, is incorporated into the non-perturbative Parton Distribution Functions (PDFs).
The other scale present in the factorized cross-section in Eq. 1.1 is the renormalization scale (μ_R). Its necessity arises because the calculation of partonic interactions in QCD using Feynman diagrams often results in ultraviolet (UV) divergences. These infinities do not indicate a fundamental error in the theory, but suggest a distinction between the bare parameters in the Lagrangian and physically observable quantities. The process of renormalization allows us to absorb these divergences into a redefinition of the Lagrangian's parameters, providing finite expressions for measurable quantities. The consequence of this procedure is that the coupling constant becomes a function of the energy scale, a phenomenon known as "running" [5]. The

renormalization scale μ_{R} is the energy at which the coupling constant is defined, thereby encapsulating the quantum corrections of the theory.
For simple processes dominated by a single characteristic energy scale μ, it is conventional to set both μ_{F} and μ_{R} equal to that scale [11]. Therefore, throughout this thesis, we set $\mu_{\mathrm{F}} = \mu_{\mathrm{R}} = \mu$. Since their exact values are arbitrary, a physical prediction (like a cross-section) must be independent of them[3].
Referring to Eq. 1.1, we can state that only the left-hand side represents a physically measurable quantity. The right-hand side, in contrast, consists of unobservable components: the parton distribution functions (PDFs), which are extracted from experimental data, and the partonic cross-section $\mathrm{d}\hat{\sigma}_{a,b}$, which is calculable within perturbation theory. It is therefore essential to understand how this latter quantity is computed.

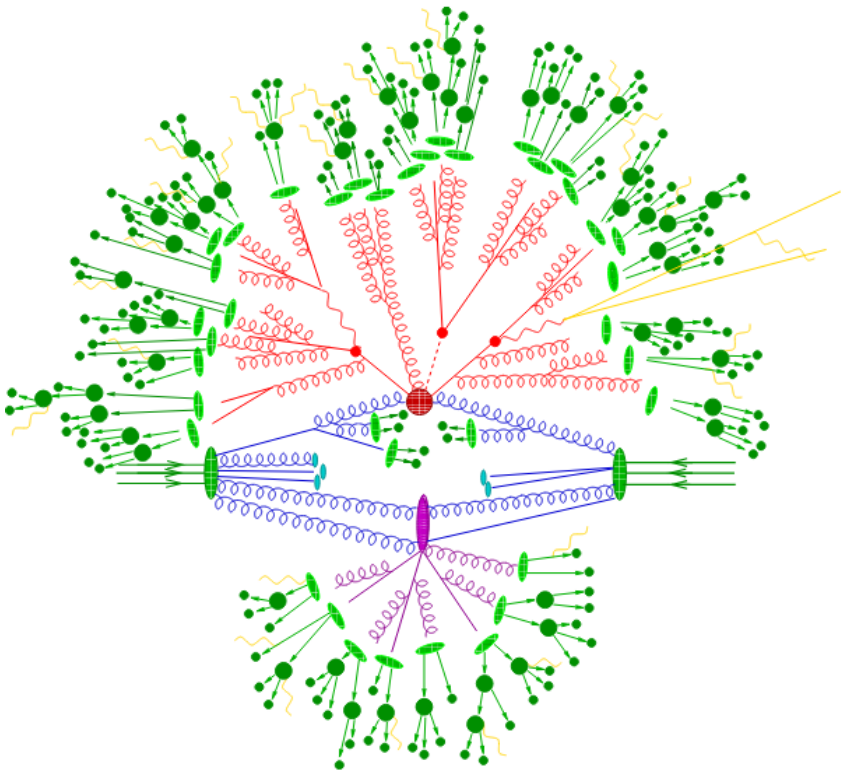

Figure 1.1: Sktetch of an hard hadron-hadron collision at a collider like the LHC. The central red blob represents the hard interaction, a high-energy collision between two partons, calculable using perturbative QCD. The incoming and outgoing partons emit initial-state (blue) and final-state (red) radiation, producing many secondary particles. Softer underlying event activity (purple) arises from additional partonic interactions within the protons. A key feature is the hierarchy of energy scales: the hard process occurs at high energies ($Q > \Lambda_{\mathrm{QCD}}$), while subsequent radiation and hadronization (green) take place at progressively lower scales, eventually transitioning to non-perturbative physics around Λ_{QCD}. Figure from [9].

[3]However, cross-sections calculated within fixed-order perturbative expansions exhibit a dependence on both the renormalization and factorization scales, μ.

§1.2.2 Partonic cross-section

We consider the inclusive[4] production of N jets at a hadron collider, together with a color-neutral system X

$$pp \to X + N\,\text{jets}\,. \tag{1.2}$$

The partonic cros section $\mathrm{d}\hat{\sigma}_{a,b}$ in Eq. 1.1 can be expanded in powers of the strong and the electroweak coupling constants, α_S and α,

$$\mathrm{d}\hat{\sigma}_{a,b} = \mathrm{d}\hat{\sigma}_{a,b}^{(0,0)} + \alpha_s \mathrm{d}\hat{\sigma}_{a,b}^{(1,0)} + \alpha_s^2 \mathrm{d}\hat{\sigma}_{a,b}^{(2,0)} + \alpha_s^3 \mathrm{d}\hat{\sigma}_{a,b}^{(3,0)} + \alpha \mathrm{d}\hat{\sigma}_{a,b}^{(0,1)} + \alpha\alpha_s \mathrm{d}\hat{\sigma}_{a,b}^{(1,1)} + \dots . \tag{1.3}$$

Due to the different values of the coupling constants, at the same order they have a different impact on the final result: at NLO, QCD corrections account for 10%, while EW account for 1%; at NNLO, QCD corrections account for 1%. Throughout this thesis, we will focus on the calculation of NLO QCD corrections.
The first term in this expansion $\mathrm{d}\hat{\sigma}_{a,b}^{(0,0)} \equiv \mathrm{d}\hat{\sigma}_{a,b}^{\mathrm{LO}}$ is called Leading Order (LO), and it is defined as [15]

$$2s_{a,b}\,\mathrm{d}\hat{\sigma}_{a,b}^{\mathrm{LO}} = \langle F_{\mathrm{LM}}^{ab}[\dots]\rangle = \mathcal{N}\int \mathrm{d}\Phi (2\pi)^4 \delta^{(4)}(p_{\mathcal{H}_\{} + p_X - p_a - p_b)\left|\mathcal{M}_0(p_a, p_b; p_{\mathcal{H}_f}, p_X)\right|^2 \mathcal{O}(p_\mathcal{H}, p_X). \tag{1.4}$$

With $\mathcal{H}_f$, we denote the list of final-state resolved particles, and $p_{\mathcal{H}_f}$ is their momentum, while p_X denotes the momentum of the color-singlet in the hard process. $\mathcal{N}$ is a normalization factor: it takes into account color and spin averages as well as symmetry factors. With $s_{a,b}$, we express the partonic center-of-mass energy squared: $s = (p_a + p_b)^2 = 2p_a \cdot p_b$, considering massless partons. The matrix element for the considered process is denoted by $\mathcal{M}_0$, and $\mathcal{O}$ represents an infrared-safe observable that ensures the final state contains at least N resolved jets. This latter feature is crucial because infrared dynamics are non-perturbative and, consequently, cannot be described by an expansion in α_s. Finally, $\mathrm{d}\Phi$ is the Lorentz-invariant phase space for the final-state particles.

$$\mathrm{d}\Phi = \prod_{i=3}^{N_p}[\mathrm{d}p_i], \qquad [\mathrm{d}p_i] = \frac{\mathrm{d}^3 p_i}{(2\pi)^3 2E_i}, \tag{1.5}$$

where $N_p = N + 2$ is the number of initial- and final-state partons, and $[\mathrm{d}p_i]$ is the phase-space element of a final-state parton i. Moreover, in Eq. 1.4, summation over spins and colors of final-state partons, and averaging over spins and colors of initial-state partons are assumed.
The function F_{LM}^{ab} that appears in Eq. 1.4 is defined as in Section 2 of [14]

$$F_{\mathrm{LM}}^{ab} = \mathrm{dLips}_X |\mathcal{M}_0|^2\,\mathcal{O}, \tag{1.6}$$

where dLips_X is the Lorentz-invariant phase space for the colorless particle X, including the momentum-conserving delta function. The integration over the final-state phase space of Eq. 1.6, denoted with the angular brackets $\langle\dots\rangle$, gives exactly Eq. 1.4.
At Leading Order (LO), calculations are performed directly. The tree-level matrix elements can be computed easily using helicity techniques and colour-subamplitude decompositions [3],

[4] The inclusive cross-section counts every collision event that creates a specific particle, whether it appears alone, with jets, or with any other additional radiation. It gives the total production rate, ignoring the details of what else is produced alongside it.

and are then integrated, either numerically or analytically.
The strong coupling constant in hard scattering processes is small enough to allow for a perturbative description, but not enough to make higher-order corrections entirely negligible. Therefore, in order to claim high precision, we also need to compute QCD corrections. In this way, results are obtained that also include long-distance effects. The NLO correction $\mathrm{d}\hat{\sigma}_{a,b}^{(1,0)} \equiv \mathrm{d}\hat{\sigma}_{a,b}^{\mathrm{NLO}}$ to a partonic cross section consists of three terms: the one-loop (virtual) contribution, the real emission contribution, and the contribution related to parton distribution functions

$$\mathrm{d}\hat{\sigma}_{a,b}^{\mathrm{NLO}} = \mathrm{d}\hat{\sigma}_{a,b}^{\mathrm{V}} + \mathrm{d}\hat{\sigma}_{a,b}^{\mathrm{R}} + \mathrm{d}\hat{\sigma}_{a,b}^{\mathrm{pdf}}. \tag{1.7}$$

The last term, $\mathrm{d}\hat{\sigma}_{a,b}^{\mathrm{pdf}}$, is generated by the renormalization of the PDFs at LO, and its expression is known [6]. The other terms, $\mathrm{d}\hat{\sigma}_{a,b}^{\mathrm{V}}$ and $\mathrm{d}\hat{\sigma}_{a,b}^{\mathrm{R}}$, are related to either the emission of an additional leg in the Feynman diagram, i.e., an extra parton in the final state (real correction), or to the emission and reabsorption of a parton through a loop (virtual correction).

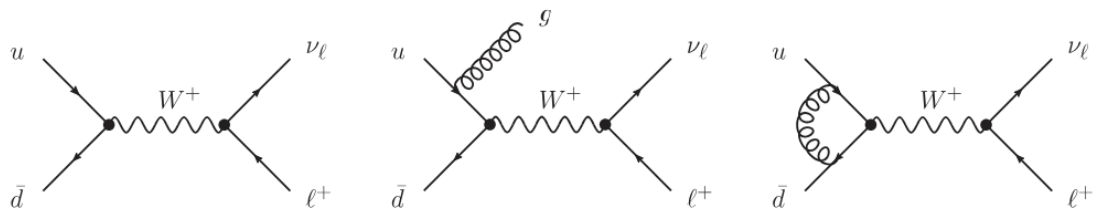

Figure 1.2: Feynman diagrams for W boson production at hadron colliders. The diagram on the left corresponds to the leading-order (LO) calculation of the total cross-section. The diagrams shown in the middle and on the right represent the real and virtual corrections, respectively, which together constitute the next-to-leading-order (NLO) contributions to the total cross-section. Figure from [11]
.

It is important to emphasize that the distinction between real and virtual corrections has no intrinsic physical meaning: it is not meaningful to speak of "virtual" or "real" radiation. This division is instead a computational tool, introduced to organize the calculation and manage the various contributions more effectively.
The treatment of these terms is non-trivial, as they exhibit divergences in specific energy regimes. The virtual contributions, for instance, contain ultraviolet (UV) singularities. These are removed through the process of renormalization[5], a procedure that ensures physical observables, when expressed in terms of appropriately defined renormalized parameters, become insensitive to the high-energy UV region.
Furthermore, the low-momentum (soft) and small-angle (collinear) kinematic regions produce singularities in both the real and virtual contributions. These infrared (IR) singularities are not independent: the real and virtual corrections are fundamentally linked by their infrared behavior. The divergence of scattering amplitudes in the soft or collinear limit means these kinematic configurations provide the dominant contributions to cross-sections. Consequently, a precise and careful estimation of these limits of QCD amplitudes is of highest importance.

[5]Throughout this thesis, we work with UV-renormalized matrix elements.

§1.2.3 Infrared poles and their cancellation

In order to deal with IR divergences, it is convenient to employ dimensional regularization [2]. This technique involves the analytical continuation of momentum space from 4 to $d = 4 - 2\epsilon$ dimensions, where $\epsilon \in \mathbb{C}$ and $\mathrm{Re}(\epsilon) < 0$. In this framework, divergences that manifest as $1/0$ poles in four dimensions instead appear as poles in $1/\epsilon$ in the complex dimensional plane.
The virtual corrections $\mathrm{d}\hat{\sigma}^{\mathrm{V}}_{a,b}$ contain explicit infrared and collinear poles and are independent of the details of the hard matrix element [6]. In contrast, the real emission contribution $\mathrm{d}\hat{\sigma}^{\mathrm{R}}_{a,b}$ contains kinematic singularities that only become explicit $1/\epsilon$ poles upon integration over the phase space of the additional final-state parton. However, we must avoid a naive integration over the entire radiation phase space, as it would render the cross section inclusive rather than differential, discarding all information on the kinematics of the radiated parton. This information is often crucial since jet properties provide essential information for defining experimental signatures.
We therefore require a method to extract the implicit $1/\epsilon$ poles from the real emission contributions without performing this integration. The key insight that allows us to overcome this obstacle is that, in singular kinematic regions, real emissions are always unresolved, meaning they lack a distinct experimental signature. Consequently, we can safely integrate over the singular regions of their phase space without losing any physically observable information.
Once the $1/\epsilon$ poles are extracted from both the virtual and real corrections, their sum is guaranteed to be free of infrared divergences due to the Bloch-Nordsieck [1] and Kinoshita-Lee-Nauenberg theorems.
Over time, various methods have been developed to perform fully differential QCD computations for hadron collider processes, both at NLO and NNLO. Many of these approaches, however, are extremely complex, non-transparent, and require significant CPU time to produce stable results. Among the existing methods, the one that most closely meets the criteria for an optimal solution is the Nested Soft-Collinear (NSC) Subtraction Scheme [10], which will be detailed in Chapter 2. The numerical stability and computational efficiency of this method can, however, be further improved. A step forward in this direction will be presented in Chapter 3; this represents the original contribution of this thesis.
Before entering into the details of the NSC Subtraction Scheme and its potential improvement, it is useful to first explore the origin of IR divergences in more depth and examine the specific structure of the infrared limit of NLO QCD amplitudes.

§1.2.4 The origin of infrared divergences in real-emission contributions

QCD amplitudes for real emission processes become singular in kinematic limits where the emitted massless parton, a gluon or a quark, becomes soft (low energy) or is emitted collinearly to another parton (gluon, quark or anti-quark). In these limits, the propagator of the emitted particle approaches its on-shell condition, leading to divergent behavior.
To show explicitly these divergences, we must first express the phase-space integration measure (before applying dimensional regularization) in hyperspherical coordinates, considering the emitted massless particles ($|\mathbf{p}_i| = E_i$, $|\mathbf{p}_i|^2 = 0$)

$$[\mathrm{d}p_{\mathfrak{m}}] \sim \mathrm{d}E_{\mathfrak{m}} E_{\mathfrak{m}} \mathrm{d}\theta_{i\mathfrak{m}} \sin\theta_{i\mathfrak{m}} \tag{1.8}$$

where $\mathfrak{m}$ indicates the unresolved parton, and i is another parton in the process.
First, we consider the case where the emitted particle $\mathfrak{m}$ is a gluon. To obtain the real radiation

corrections, we integrate the squared absolute value of the amplitude $|\mathcal{M}|^2$ for the process under consideration. The energy integral has limits from 0 to $E_{\max}$ (which is defined by energy conservation), and the angular integral has limits from 0 to π. Since this integral becomes singular in the limits $E_m \to 0$ (soft) and $\theta_{i\mathfrak{m}} \to 0$ (collinear), we must examine the behavior of the amplitude in these regimes.
For a generic QCD amplitude $\mathcal{M}$ involving n partons with four-momenta $p_1, p_2, \ldots, p_n$ and an additional soft gluon with vanishing four-momentum $p_{\mathfrak{m}}$, the squared amplitude factorizes into (i) the squared amplitude for the hard process without the gluon and (ii) an eikonal factor that depends only on the color charges and momenta of the hard partons and the momentum of the soft gluon ($p_{\mathfrak{m}}$) [7]

$$\lim_{E_{\mathfrak{m}}\to 0} |\mathcal{M}(p_1, p_2, \ldots, p_n; p_{\mathfrak{m}})|^2 = -4\pi\alpha_s\mu^{2\epsilon} \sum_{i,j=1}^{n} \mathcal{S}_{ij}(p_{\mathfrak{m}})\vec{T}_i \cdot \vec{T}_j |\mathcal{M}_0(p_1, p_2, \ldots, p_n)|^2, \tag{1.9}$$

where the general eikonal factor is

$$\mathcal{S}_{ij}(p_{\mathfrak{m}}) = \frac{p_i \cdot p_j}{(p_i \cdot p_{\mathfrak{m}})(p_j \cdot p_{\mathfrak{m}})} \sim \frac{1}{E_{\mathfrak{m}}^2} \tag{1.10}$$

and the square of the color charges are $\vec{T}_i^2 = C_F$ if i is a quark or an anti-quark, and $\vec{T}_i^2 = C_A$ if i is a gluon.
Therefore, the energy integral does not converge for soft gluon emissions in any process

$$\int_0^{E_{\max}} \frac{\mathrm{d}E_{\mathfrak{m}}}{E_{\mathfrak{m}}} \to \infty \tag{1.11}$$

Whereas, in the collinear limit, i.e., the limit where a gluon is emitted parallel to a quark, the amplitude-squared factorizes into (i) a splitting function, which describes the probability for the quark to radiate the gluon collinearly at a given energy, and (ii) the squared hard amplitude, which now depends on the resulting quark momentum after the emission.

$$\lim_{\theta_{i\mathfrak{m}}\to 0} |\mathcal{M}(p_1, \ldots, p_n; p_{\mathfrak{m}})|^2 \sim P_{f_{[i\mathfrak{m}]}f_i} |\mathcal{M}_0(p_1, \ldots, p_n)|^2 \sim \frac{1}{(p_i - p_{\mathfrak{m}})^2} \sim (1 - \cos(\theta_{i\mathfrak{m}}))^{-1} \sim \theta_{i\mathfrak{m}}^{-2} \tag{1.12}$$

so, even the angular integral for real emissions does not converge

$$\int_0^{\pi} \frac{\mathrm{d}\theta_{i\mathfrak{m}}}{E_{\theta_{i\mathfrak{m}}}} \to \infty. \tag{1.13}$$

The unresolved parton $\mathfrak{m}$ could also be a quark or an antiquark. However, the emission of a soft quark leads to a convergent integral; consequently, no divergences are associated with soft quark or antiquark emissions. Divergences do arise in the collinear limit, but, as in the gluon case, the amplitude factorizes into a hard process involving a parton with rescaled momentum and a corresponding splitting function.
It is important to consider the origin of these infinities. The presence of divergences is, in fact, a manifestation of long-distance effects: they signal that non-perturbative contributions are entering our perturbative calculation. This could be a problem, as we lack methods to treat non-perturbative QCD effects from first principles [12]. Fortunately, as stated in the previous

section, the divergences emerging from the real and virtual corrections cancel when summed together. Therefore, perturbative QCD corrections remain insensitive to the details of infrared physics.
However, achieving the cancellation of the $1/\epsilon$ poles by simply summing the real and virtual corrections is not straightforward. This complication arises because the virtual corrections are defined in an n-particle phase space, whereas the real corrections inhabit an $(n+1)$-particle phase space. This mismatch in the dimensionality of the integration domains is precisely the reason why dedicated subtraction schemes are required.

Chapter 2

NLO QCD corrections in the NSC Subtraction Scheme

The Nested Soft-Collinear Subtrasction Scheme was introduced in Ref. [10]

§2.1 Draft

Chapter 3

NLO QCD corrections with θ-parameters in the NSC Subtraction Scheme

§3.1 Draft

Appendices

Appendix A

Draft appendix

§A.1 Draft

Lorem ipsum dolor sit amet [**pauli**].

Bibliography

[1] F. Bloch and A. Nordsieck. "Note on the Radiation Field of the Electron". Phys. Rev. **52** (1937), pp. 54–59. DOI: 10.1103/PhysRev.52.54.

[2] G. 't Hooft. "Dimensional regularization and the renormalization group". Nuclear Physics B **61** (1973), pp. 455–468. ISSN: 0550-3213. DOI: https://doi.org/10.1016/0550-3213(73)90376-3.

[3] Guido Altarelli and G. Parisi. "Asymptotic Freedom in Parton Language". Nucl. Phys. B **126** (1977), pp. 298–318. DOI: 10.1016/0550-3213(77)90384-4.

[4] John C. Collins and Davison E. Soper. "The Theorems of Perturbative QCD". Ann. Rev. Nucl. Part. Sci. **37** (1987), pp. 383–409. DOI: 10.1146/annurev.ns.37.120187.002123.

[5] R. K. Ellis et al. *QCD and Collider Physics*. **8**. Cambridge Monographs on Particle Physics, Nuclear Physics and Cosmology. Cambridge: Cambridge University Press, 1996, p. 435. DOI: 10.1017/CBO9780511628788.

[6] S. Catani and M. H. Seymour. "A General algorithm for calculating jet cross-sections in NLO QCD". Nucl. Phys. B **485** (1997). [Erratum: Nucl.Phys.B 510, 503–504 (1998)], pp. 291–419. DOI: 10.1016/S0550-3213(96)00589-5. arXiv: hep-ph/9605323.

[7] Stefano Catani and Massimiliano Grazzini. "Infrared factorization of tree level QCD amplitudes at the next-to-next-to-leading order and beyond". Nucl. Phys. B **570** (2000), pp. 287–325. DOI: 10.1016/S0550-3213(99)00778-6. arXiv: hep-ph/9908523.

[8] Gavin P. Salam. "Towards Jetography". Eur. Phys. J. C **67** (2010), pp. 637–686. DOI: 10.1140/epjc/s10052-010-1314-6. arXiv: 0906.1833 [hep-ph].

[9] Stefan Höche. "Introduction to parton-shower event generators". arXiv preprint **arXiv:1411.4085** (2014). Lectures presented at TASI 2014. 40 pages, 12 figures. URL: https://arxiv.org/abs/1411.4085.

[10] Fabrizio Caola, Kirill Melnikov, and Raoul Röntsch. "Nested soft-collinear subtractions in NNLO QCD computations". Eur. Phys. J. C **77**.4 (2017), p. 248. DOI: 10.1140/epjc/s10052-017-4774-0. arXiv: 1702.01352 [hep-ph].

[11] John Campbell, Joey Huston, and Frank Krauss. *The Black Book of Quantum Chromodynamics : a Primer for the LHC Era*. Oxford University Press, 2018. DOI: 10.1093/oso/9780199652747.001.0001.

[12] K. Melnikov. "Lectures on QCD for hadron colliders". *Proceedings of the 2017 European School of High-Energy Physics, Evora, Portugal, 6–19 September 2017*. Ed. by M. Mulders and G. Zanderighi. Vol. 3/2018. CERN Yellow Reports: School Proceedings. CERN-2018-006-SP. Geneva: CERN, 2018. DOI: 10.23730/CYRSP-2018-003.37.

[13] K. Asteriadis. "Application of the nested soft-collinear subtraction scheme to the description of deep inelastic scattering". PhD Thesis. Karlsruhe Institute of Technology (KIT), Institute for Experimental Particle Physics (EKP), 24, 2020, p. 216. DOI: 10.5445/IR/1000135340.

[14] Federica Devoto et al. "A fresh look at the nested soft-collinear subtraction scheme: NNLO QCD corrections to N-gluon final states in $q\overline{q}$ annihilation". JHEP **02** (2024), p. 016. DOI: 10.1007/JHEP02(2024)016. arXiv: 2310.17598 [hep-ph].

[15] Federica Devoto et al. "Integrated subtraction terms and finite remainders for arbitrary processes with massless partons at colliders in the nested soft-collinear subtraction scheme" (2025). arXiv: 2509.08594 [hep-ph].